Wavelet Analysis of the Geomagnetic Field Within Source Regions of Ionospheric and Magnetospheric Currents

Michael Bayer*, Willi Freeden† , Thorsten Maier

University of Kaiserslautern
Laboratory of Technomathematics
Geomathematics Group
67653 Kaiserslautern
P.O. Box 3049
Germany
phone: ++49 631 205-3867
fax: ++49 631 29081
email: freeden@mathematik.uni-kl.de
www: http://www.mathematik.uni-kl.de/∼wwwgeo

September 30, 1999

Abstract

A multiscale method is introduced using spherical (vector) wavelets for the computation of the earth's magnetic field within source regions of ionospheric and magnetospheric currents. The considerations are essentially based on two geomathematical keystones, namely (i) the Mie representation of solenoidal vector fields in terms of toroidal and poloidal parts and (ii) the Helmholtz decomposition of spherical (tangential) vector fields. Vector wavelets are shown to provide adequate tools for multiscale geomagnetic modelling in form of a multiresolution analysis, thereby completely circumventing the numerical obstacles caused by vector spherical harmonics. The applicability and efficiency of the multiresolution technique is tested with real satellite data.

Key Words: Mie representation, Helmholtz decomposition, vector wavelets, multiresolution analysis, geomagnetic field modelling from MAGSAT data.

*The support by 'Stiftung Rheinland–Pfalz für Innovation' is gratefully acknowledged.

†Author to whom correspondence should be addressed.

1 Introduction

The near–earth magnetic field is due to three sources: (i) the *core field*, generated by geodynamic processes in the earth's core, (ii) the *crustal field*, mainly due to permanently magnetized rocks in the earth's crust, and (iii) the *external field*, generated by ionospheric and magnetospheric current systems. Modelling of the components of the geomagnetic field is of paramount importance for several applications. For example, naval and aeroplane navigation systems as well as spacecraft attitude control make excessive use of modern geomagnetic field models, exploration techniques rely on geomagnetic information to steer drilling heads for bore holes. In physics, applications include studies of the earth's structure and dynamics, calculation of radiation belts and cosmic particle orbits, investigations of solar–terrestrial interrelationships, etc. All these applications depend seriously on the geomagnetic reference field under consideration.

To a first approximation the International Geomagnetic Reference Field (IGRF) in terms of spherical harmonics is a frequently used geophysical model. This approach, basically introduced by C.F. Gauss (1836) and therefore named *Gauss representation*, however, assumes the near–earth magnetic field to be curl–free, which in connection with Maxwell's equations means that no electric current densities must be present at the place where the observations are taken. As far as earth-bound or low-atmosphere modelling is performed this assumption is certainly true, since the sources of the geomagnetic field, i.e. the electric current densities, are located within the earth's body as well as in the ionosphere and magnetosphere. In other words, the geomagnetic field 'in the space between' may be simply understood to be a *gradient field*. Conventionally, the potential is developed by means of outer and inner harmonic representations, reflecting the external and internal parts of the magnetic field corresponding to the field sources (see, for example, Backus et al. (1996), Langel (1987)). In particular, reconstruction by outer and inner harmonics remains an important technique whenever attempts of separate main field modelling, i.e. core and crustal field modelling are of interest. But also other mathematical techniques of main field modelling have been introduced. For example, in analogy to the approach in earth's gravitational potential determination (cf. Freeden (1981)), spline concepts of main field modelling have been proposed by Shure et al. (1982). *Spline approximation*, however, requires solving a square system of equations with dimension equal to the number of data. Thus the normal equation matrix will generally be a full marix, reflecting the particular status of decorrelation guaranteed by the a priori chosen kernel function (in statistical nomenclature called covariance function). This problem causes numerical difficulties with the presently available large data sets. To some extend, indeed, the difficulties may be overcome by several techniques (for example, fast summation, panel clustering (see e.g. Freeden et al. (1999))), but the numerical obstacles are the main reasons why approximation methods based on (single scale) spline procedures could not keep pace with the increasing flow of observational information. The serious drawback of spline interpolation and/or spline smoothing of geomagnetic data is that it only provides a single scale modelling by use of a (fixed) kernel (covariance) function. In conclusion, there is no efficient transition from global to local modelling by only using one kernel (covariance) function with (fixed) space/frequency localization property.

For future work, however, large innovations have to be made in geomagnetic modelling from satellite data. The reasons for this statement are of physical and numerical nature:

Physical constraints: Satellite missions (like MAGSAT or CHAMP) collect their data within the

ionosphere that is a source region of the geomagnetic field. Consequently, satellite data of low orbiting satellites do not meet the prerequisites for the Gauss representation. The magnetic field, measured by satellites in the ionosphere, is no longer a gradient field. In fact, it also contains magnetic contributions from current densities on the satellite's track. But this means that new vectorial methods, not based on the existence of a scalar potential, must be derived in close orientation on a (quasi–static) formulation of Maxwell's equations (in the form of pre–Maxwell's equations). Well–known from the literature (cf. Backus et al. (1996) and the references therein) is the resolution of the magnetic field by means of the so–called *Mie representation*, i.e. the splitting into poloidal and toroidal parts. The poloidal fields are due to tangential current densities below and above the satellite's track, whereas the toroidal fields are created by radial currents which are crossing the satellite's orbit. Those radial currents and the resulting magnetic effects are more and more subject of recent research (see, for example, Olsen and Pfitzer (1974), Richmond (1974), Stern (1976), Iijima and Potemra (1978), Kisabeth (1979), Kosik (1984), Langel and Estes (1985), Donovan (1993), Langel et al. (1996), Lühr et al. (1996), Olsen (1997), Engels and Olsen (1998)). In our approach geomagnetic modelling of the magnetic field on (spherical) satellite orbits becomes available by combining the Mie representation with the *Helmholtz decomposition theorem* of the theory of vector fields on the sphere.

Numerical requirements: The remaining question is how to computationally obtain in terms of suitable trial functions (fields) the Mie representation for a given set of vectorial satellite data. The *uncertainty principle* (confer the scalar theory by Freeden and Windheuser (1997), Freeden (1998) and their generalization to the vector case by Beth (1999)) provides an adequate tool for the classification of (spherical restrictions of) poloidal and toroidal vector fields by determining a trade off between two 'spreads', one for the position (space) and the other for the momentum (frequency). The main statement is that *sharp localization in space and in frequency are mutually exclusive.* The varieties of space/frequency localization (cf. Freeden (1999)) can be illustrated by considering different poloidal and toroidal trial fields on the sphere being suitable for constructive approximation. *Vector (spherical) harmonics* show an ideal frequency localization, but no space localization. The spectrum (of band–limited and non band–limited) *kernel (covariance) functions* known from vectorial spline theory (cf. Freeden and Gervens (1991) , Freeden et al. (1998)) shows all intermediate cases of space/frequency localization. But in view of the amount of space/frequency localization it is also worth distinguishing bandlimited from non–bandlimited kernels. As a matter of fact, it turns out that non–bandlimited kernels show a much stronger space localization than their comparable band–limited counterparts. Finally, the *Dirac kernels* show ideal space localization, but no frequency localization. Thus they provide the final stage in the spatial resolution of the magnetic field by trial functions. In conclusion, vector harmonics and Dirac kernels are 'extreme trial functions' for purposes of geomathematical modelling.

The classification of trial fields by the uncertainty principle for approximating the Mie representation from discrete vectorial data, therefore, leads us to the following philosophy of constructive approximation (cf. Freeden (1999)): It is canonical to start the approximation of the geomagnetic field with non-space localizing and ideally frequency localizing vector spherical harmonics to determine a trend approximation, i.e. the long wavelength contribution. For the intermediate cases between long and short wavelength approximation we have to continue with appropriately balanced space/frequency (bandlimited) kernel functions. Finally, non-bandlimited kernel functions have to come into play to analyse seriously space localizing, i.e. short wavelengh phe-

nomena.

The *essential feature of wavelets* as presented in this paper is their ability to realize multiscale approximations of the magnetic field in form of a *multiresolution analysis*. By using a mathematically well–structured sequence of more and more kernel (covariance) functions reflecting the various levels of space/frequency localization, the reference space, i.e. the space of square–integrable vector fields is decomposed into a nested sequence of approximating subspaces (scale spaces) representing the different stages of *decorrelation*. In doing so wavelets are used as physically motivated mathematical means for breaking up a complicated vector field such as the near–earth magnetic field into many simple pieces of different scales and positions. This multiscale approach allows tree algorithms and compression of data (which is impossible in the case of non-space localizing vector harmonics). The particular efficiency of wavelets is caused by the property that only a few wavelet coefficients in the wavelet table are needed in areas where the magnetic field is 'smooth', while stronger resolution of a complicated pattern is settled by a *zooming–in capability* using more and more space–localizing wavelets. *Fast computation* becomes available in form of pyramid schemata. This enables numerical evaluation for large data sets such as real satellite data sets.

The outline of the paper is as follows: Chapter 2 presents a brief description of the physical framework. Chapter 3 is concerned with the Mie representation. Chapter 4 demonstrates its application to the geomagnetic field. Chapter 5 recapitulates the Helmholtz theorem for spherical vector fields. The definition of vector spherical harmonics is given in Chapter 6. Chapter 7 deals with kernel functions (briefly called kernels) in the (reference) space of square–integrable vector fields on the sphere. In Chapter 9, the approximation of spherical vector fields is guaranteed by an approximate convolution identity in terms of vectorial scaling functions. This assumes the adequate formulation of convolutions (in Chapter 8). Next, in Chapter 10, we define vector wavelets on the sphere. A characterization of their main properties is presented. Some examples of bandlimited and non-bandlimited wavelets are listed in Chapter 11. Graphical illustrations are given for the non-bandlimited Abel–Poisson wavelet and the bandlimited Shannon and CUP wavelet. Finally, the separation of poloidal and toroidal geomagnetic field components from MAGSAT data via vectorial multiresolution analysis is shown using bandlimited CUP–wavelets (in Chapter 12).

2 Physical Framework

We start our considerations with a short note on notation: The standard notation in this paper is such that capital letters F, G, etc. denote scalar functions. Vector fields are represented by lower-case letters f, g, etc.

As is well–known, macroscopic electrodynamics is the theoretical basis for dealing with the subject of geomagnetism. The fundamental equations governing that branch are Maxwell's equations for polarizable media. Neglecting the influence of Maxwell's displacement current density (cf. Backus et al. (1996)), results in two major advantages. First, the equations decouple completely and - as far as the magnetic field is concerned - it suffices to look at the static

equations (i.e. the pre–Maxwell equations)

$$\nabla \cdot b = 0, \tag{1}$$

$$\nabla \wedge b = \mu_0 j, \tag{2}$$

where b (in classical geophysical notation usually denoted by $\vec{B}$) is the magnetic induction, i.e. the magnetic field, and μ_0 is the vacuum permeability, $\mu_0 = 4\pi \cdot 10^{-7}\mathrm{VsA}^{-1}\mathrm{m}^{-1}$. Note that the electric current density j is of zero divergence, i.e.

$$\nabla \cdot j = 0. \tag{3}$$

This fact will be of significant importance later on.

Earlier concepts in geomagnetic modelling assume that the geomagnetic data are solely collected within a spherical shell $\Omega_{(\rho,\sigma)}$ around the origin – with inner radius ρ and outer radius σ – between the earth's surface and the ionosphere so that the current density j can be neglected. This results in $\nabla \wedge b = 0$, $\nabla \cdot b = 0$ which implies that there exists a scalar potential U in $\Omega_{(\rho,\sigma)}$ such that $b = -\nabla U$ and $\Delta U = 0$ in $\Omega_{(\rho,\sigma)}$. In order to model the magnetic field b the potential is expanded into a Fourier series of (scalar) spherical harmonics (multipole expansion), and the expansion coefficients are chosen such that the gradient of the potential fits – in the sense of a least–square metric – the given vectorial data as good as possible. This method, which is known as Gauss representation, has been used and constantly improved for more than 150 years now, so that profound numerical and theoretical techniques are existent (see e.g. Langel et al. (1996) for up to date results).

With modern satellite missions like CHAMP, however, the situation changes. The data are acquired within the ionosphere, where $j = 0$ is no longer a valid assumption in the pre–Maxwell equations. All over the magneto- and ionosphere various current systems are present and their corresponding magnetic fields contribute to the geomagnetic one. The most important ionospheric current systems are the so-called *equatorial electro jet (EEJ)* as well as the so-called *field aligned currents*. Due to the intense solar radiation on the earth's dayside (i.e. the hemisphere directed to the sun) the electric conductivity of the ionosphere is increased and tidal forces, due to solar heating as well as solar and lunar attraction, can drive large current systems. In connection with polarization effects in the ionospheric plasma the geomagnetic field produces an enhanced hall conductivity (Cowling Effect) in the vicinity of the geomagnetic equator. This increased conductivity results in an amplified current system - the EEJ - flowing roughly along the magnetic equator. As regards our later considerations it is worth mentioning that the EEJ, though mainly tangential, also provides a notable radial current density. Currents flowing along the geomagnetic field lines - the field aligned currents - are caused by magnetospheric and ionospheric coupling or imbalances of Sq-current systems (see e.g. Olsen (1997) and the references therein). In the polar regions field aligned currents flow onto or away from the earth's body, thus contributing large radial current densities confined to these areas. The EEJ and the field aligned currents are of importance for modern day ionospheric satellite missions, since the corresponding magnetic effects cannot be modelled via the Gauss representation. With the current density not being negligible anymore, the existence of a scalar magnetic potential can no longer be guaranteed.

3 Mie Representation

Backus (1986), Backus et al. (1998) describe a more general mathematical theory for the decomposition of vector fields into so-called poloidal and toroidal parts. This so-called *Mie-representation* can be applied to geomagnetic vector data from magnetic source regions and will turn out to be a generalization of the Gauss representation. In what follows we will briefly introduce the Mie representation.

For later use we define the operator Λ given by $\Lambda_x = x \wedge \nabla_x$, $x \in \mathbb{R}^3$. The Mie representation deals with the decomposition of solenoidal vector fields. A vector field v defined on $\Omega_{(\rho,\tau)}$, $0 < \rho < \sigma < \tau < \infty$, is called *solenoidal* if, for every closed surface S being entirely in $\Omega_{(\rho,\tau)}$, the surface integral $\int_S v \cdot \nu \, ds$ vanishes (ν is the normal on S pointing into the exterior of the inner space of S). Note that if v is solenoidal in $\Omega_{(\rho,\tau)}$, then $\nabla \cdot v = 0$ in $\Omega_{(\rho,\tau)}$, whereas the converse is – in general – wrong (cf. Backus et al. (1996)). From Eq. (1) we deduce that the geomagnetic field is divergence free in the whole space $\mathbb{R}^3$ and, therefore, (by means of Gauss' theorem) is solenoidal in $\mathbb{R}^3$. Hence, the application of the Mie representation to the geomagnetic field is justified.

A vector field t is called *toroidal* in $\Omega_{(\rho,\tau)}$ if there is a scalar field Q such that $t = \Lambda Q$ in $\Omega_{(\rho,\tau)}$. Q is called the *toroidal scalar*. A vector field p is called *poloidal* in $\Omega_{(\rho,\tau)}$ if there is a scalar field P such that $p = \nabla \wedge \Lambda P$ in $\Omega_{(\rho,\tau)}$. P is called the *poloidal scalar*.

The Mie representation theorems (cf. Backus et al. (1996)) now read as follows:

(i) Let $\Omega_{(\rho,\tau)}$ be a spherical shell with $0 < \rho \leq \sigma < \tau < \infty$. Furthermore, let v be a solenoidal vector field in $\Omega_{(\rho,\tau)}$ Then there exist *unique* scalar fields P, Q in $\Omega_{(\rho,\tau)}$ such that

$$\int_{\Omega_r} Q(x) d\omega_r(x) = \int_{\Omega_r} P(x) d\omega_r(x) = 0, \quad r \in (\rho, \tau),$$

and

$$v = \nabla \wedge \Lambda P + \Lambda Q$$

in $\Omega_{(\rho,\tau)}$.

(ii) Suppose that v is a solenoidal vector field in a spherical shell $\Omega_{(\rho,\tau)}$ with $0 < \rho < \sigma < \infty$, then there exist a *unique* poloidal field p and a *unique* toroidal field t such that $v = p + t$ holds true in $\Omega_{(\rho,\tau)}$.

Consequently the Mie representation is unique, and whatever technique is used to obtain this decomposition it is clear that the corresponding poloidal and toroidal fields are uniquely determined. These results are the basis for our further considerations.

4 Application to the Geomagnetic Field

Let b be a vector field solenoidal in $\Omega_{(\rho,\tau)}$ with the Mie representation

$$b = \nabla \wedge \Lambda P_b + \Lambda Q_b = p_b + t_b \tag{4}$$

where P_b and Q_b are sufficiently often differentiable in $\Omega_{(\rho,\tau)}$. Moreover, let j be a vector field in the spherical shell $\Omega_{(\rho,\tau)}$ satisfying the equations $\nabla \cdot j = 0$ and

$$\nabla \wedge b = \lambda j, \quad \lambda \in \mathbb{R} \setminus \{0\}\,. \tag{5}$$

Combining (4) and (5) a straightforward calculation leads to $j = \frac{1}{\lambda}\left(\nabla \wedge \Lambda Q_b - \Lambda(\Delta P_b)\right)$ in $\Omega_{(\rho,\tau)}$. But this just shows that j is also solenoidal, and we have $j = \nabla \wedge \Lambda P_j - \Lambda Q_j$ in $\Omega_{(\rho,\tau)}$,where the poloidal and toroidal scalars P_j and Q_j, respectively, are given by

$$P_j = \frac{1}{\lambda} Q_b, \tag{6}$$

$$Q_j = \frac{1}{\lambda} \Delta P_b. \tag{7}$$

Hence, by determining the Mie scalars of b (e.g. the magnetic field) we also determine the Mie scalars of j (e.g. the electric current density j). Furthermore, with some additional mathematical effort it can be deduced (cf. Backus et al. (1996)) that for the solenoidal vector field j (and for any other solenoidal vector field) in $\Omega_{(\rho,\tau)}$ its radial projection is only connected with its poloidal field scalar P_j via the identity

$$\frac{x}{|x|} \cdot j(x) = j_{rad}(x) = \frac{1}{|x|}\left(\Delta P_j\right)(x), \quad x \in \Omega_r$$

(with $r \in (\rho,\tau)$). In spherical formulation using polar coordinates $x = r\xi$, $r = |x|$, $\xi = x/|x|$, $r \in (\rho,\tau)$, we are therefore confronted with the differential equation

$$r\left(\xi \cdot j_{rad}(r\xi)\right) = \left(\Delta^* P_j\right)(r\xi)\,, \tag{8}$$

where Δ^* denotes the Beltrami operator on the sphere Ω_r, $r \in (\rho,\tau)$. Since j is solenoidal we know that $\int_{\Omega_r} j_{rad}(r\xi)\; d\omega_r(r\xi) = 0$ and $\int_{\Omega_r} P_j(r\xi)\; d\omega_r(r\xi) = 0$. But this suffices to uniquely solve the Beltrami differential equation (8) (see e.g. Freeden et al. (1998)), and we get

$$P_j(r\xi) = \int_{\Omega_r} G(\Delta^*; r\xi, r\eta)\, r\, j_{rad}(r\eta)\; d\omega(r\eta), \quad r\xi \in \Omega_r$$

with $G(\Delta^*;\cdot,\cdot)$ being the Green function with respect to the Beltrami differential operator Δ^* (cf. Freeden and Gervens (1991)). Using (6) we can connect j_{rad} with the toroidal scalar of b as follows:

$$Q_b(r\xi) = \lambda \int_{\Omega_r} G\left(\Delta^*; r\xi, r\eta\right) r j_{rad}(r\eta) d\omega_r(r\eta), \quad r\xi \in \Omega_r\ .$$

This means that if the solenoidal vector fields b and j are connected via (5), then on each sphere Ω_r with $\sigma < r < \tau$ the toroidal field t_b is solely due to the radial projection of j.

Let now $\lambda = \mu_0$. Then the above considerations imply the following statements:

(i) Let b and j, respectively, be the magnetic field and the electric current density in a spherical shell $\Omega_{(\rho,\tau)}$. If no current crosses the sphere Ω_r with $r \in (\rho, \tau)$, that is if the radial current density j_{rad} vanishes on Ω_r, then the magnetic field b on Ω_r is purely poloidal.

(ii) Let b and j, respectively, be the magnetic field and the electric current density in a spherical shell $\Omega_{(\rho,\tau)}$. If $j = 0$ in $\Omega_{(\rho,\tau)}$, then the magnetic field in $\Omega_{(\rho,\tau)}$ is purely poloidal.

The latter result shows that the Mie representation is a generalization of the Gauss method. If we use geomagnetic data from regions with negligible current densities, the corresponding magnetic vector field can equivalently be represented as a poloidal or a gradient field. If, however, the current density is notable, the Gauss representation looses its validity and the corresponding magnetic field consists of a poloidal as well as a toroidal part.

Our results show that the toroidal magnetic field is solely due to radial current densities at the place of the measurements. Consequently, vector data from ionospheric satellite missions should show significant toroidal fields near the polar regions (due to field aligned currents) and along the geomagnetic equator (resulting from the EEJ).

There remains the question of how to extract the restrictions of poloidal and toroidal parts to a sphere from a given set of vectorial data. Olsen (1997) suggests a technique based on a spherical harmonic expansion of the toroidal and poloidal scalars. In accordance with the uncertainty principle we, however, suggest the use of kernel functions, since this method can be applied directly to given vectorial data without making the detour using scalar functions. In what follows, we briefly summarize the necessary theoretical background and show how the Mie representation and the kernel functions on the sphere can be connected in adequate manner. Observe that, by virtue of the isomorphism $\Omega_1 \ni \xi \mapsto r\xi \in \Omega_r$, we can assume vector fields $f : \Omega_r \to \mathbb{R}$, $r \in (\rho, \tau)$ to be defined on the unit sphere $\Omega (= \Omega_1)$ by $f(x) = f(r\xi), x = r\xi, \xi \in \Omega$, $r \in (\rho, \tau)$. For the sake of simplicity, we therefore restrict all our activities to the unit sphere Ω.

5 The Helmholtz Theorem

For a given vector field $f = \Omega \to \mathbb{R}^3$, the field $f_{nor} : \xi \to f_{nor}(\xi) = (\xi \cdot f(\xi))\xi$, $\xi \in \Omega$ is called the *normal part* of f, while $f_{tan} : \xi \mapsto f_{tan}(\xi) = f(\xi) - f_{nor}(\xi)$, $\xi \in \Omega$ is called the *tangential part* of f. A vector field f is called *tangential (resp. normal)*, if $f(\xi) = f_{tan}(\xi)$ (resp. $f(\xi) = f_{nor}(\xi)$) for all $\xi \in \Omega$.

The study of vector fields on the sphere can be greatly simplified in terms of the following operators: ∇^* (*surface gradient*), L^* (*surface curl gradient*), $\nabla^* \cdot$ (*surface divergence*), $L^* \cdot$ (*surface curl*), and Δ^* (*Beltrami operator*). Their representation in terms of polar coordinates and their role in integral formulas on the sphere are extensively discussed in Freeden et al. (1998). By use of these operators any vector field $f \in c^{(1)}(\Omega)$ admits the 'Helmholtz decomposition'

$$f(\xi) = f_{nor}(\xi) + f_{tan}(\xi), \qquad \xi \in \Omega\,, \tag{9}$$

where

$$\begin{aligned} f_{nor}(\xi) &= f^{(1)}(\xi), \quad \xi \in \Omega, \\ f_{tan}(\xi) &= f^{(2)}(\xi) + f^{(3)}(\xi), \quad \xi \in \Omega, \end{aligned}$$

and $f^{(1)}(\xi) \cdot f^{(i)}(\xi) = 0$, $i = 2, 3$, $\nabla_\xi^* \cdot f^{(2)}(\xi) = \nabla_\xi^* \cdot f_{tan}(\xi)$, $\nabla_\xi^* \cdot (f^{(2)}(\xi) \wedge \xi) = 0$, $\nabla_\xi^* \cdot f^{(3)}(\xi) = 0$, $\nabla_\xi^* \cdot (f^{(3)}(\xi) \wedge \xi) = \nabla_\xi^* \cdot (f(\xi) \wedge \xi)$. Due to Backus et al. (1996) there exist uniquely determined functions $F_i \in C^{(2)}(\Omega)$, $i = 2, 3$ satisfying

$$\int_\Omega F_i(\xi) d\omega(\xi) = 0, \qquad i = 2, 3\,,$$

such that

$$\begin{aligned} f^{(2)}(\xi) &= \nabla_\xi^* F_2(\xi), \quad \xi \in \Omega, \\ f^{(3)}(\xi) &= L_\xi^* F_3(\xi) = \xi \wedge \nabla_\xi^* F_3(\xi) \quad \xi \in \Omega. \end{aligned} \tag{10}$$

Freeden and Gervens (1991) give the explicit representation of F_i, $i = 2, 3$, in terms of Green's function with respect to the Beltrami operator Δ^*, namely

$$\begin{aligned} F_2(\xi) &= -\int_\Omega G\left(\Delta^*; \xi, \eta\right) \nabla_\eta^* \cdot (f(\eta) - (\eta \cdot f(\eta))\eta) \; d\omega(\eta), \\ F_3(\xi) &= -\int_\Omega G\left(\Delta^*; \xi, \eta\right) \nabla_\eta^* \cdot (\eta \wedge f(\eta)) \; d\omega(\eta). \end{aligned}$$

Using the operators $O^{(i)} : c^{(1)}(\Omega) \to C^{(0)}(\Omega)$, $i = 1, 2, 3$, defined by

$$\begin{aligned} O_\xi^{(1)} f(\xi) &= \xi \cdot f(\xi), \\ O_\xi^{(2)} f(\xi) &= -\nabla_\xi^* \cdot (f(\xi) - (\xi \cdot f(\xi))\xi)\,, \\ O_\xi^{(3)} f(\xi) &= \nabla_\xi^* \cdot (\xi \wedge f(\xi))\,, \end{aligned}$$

we are able to rewrite the decomposition formula as follows:

$$\begin{aligned} f^{(1)}(\xi) &= \left(O_\xi^{(1)} f(\xi)\right) \xi, \\ f^{(2)}(\xi) &= -\nabla_\xi^* \int_\Omega G\left(\Delta^*; \xi, \eta\right) O_\eta^{(2)} f(\eta) d\omega(\eta), \\ f^{(3)}(\xi) &= -L_\xi^* \int_\Omega G\left(\Delta^*; \xi, \eta\right) O_\eta^{(3)} f(\eta) \; d\omega(\eta). \end{aligned}$$

Corresponding to the operators $O^{(i)}$ we introduce operators $o^{(i)} : C^{(1)}(\Omega) \to c^{(0)}(\Omega)$, $i = 1, 2, 3$, by setting

$$\begin{aligned} o_\xi^{(1)} F(\xi) &= F(\xi)\xi, \\ o_\xi^{(2)} F(\xi) &= \nabla_\xi^* F(\xi), \\ o_\xi^{(3)} F(\xi) &= L_\xi^* F(\xi) = \xi \wedge \nabla_\xi^* F(\xi) \;\; . \end{aligned}$$

Then it is not difficult to show that for $F \in C^{(2)}(\Omega)$

$$O^{(j)}\left(o^{(i)}F(\xi)\right) = 0, \qquad j \neq i.$$

Moreover, for $i = j$, we get

$$\begin{aligned} O^{(1)}\left(o^{(1)}F(\xi)\right) &= F(\xi), \\ O^{(2)}\left(o^{(2)}F(\xi)\right) &= -\Delta_\xi^* F(\xi), \\ O^{(3)}\left(o^{(3)}F(\xi)\right) &= -\Delta_\xi^* F(\xi) \ . \end{aligned}$$

Taking into account the uniqueness of both the Mie and the Helmholtz representation on a sphere, it is obvious that $o_\xi^{(3)}F_3$ in (10) and hence in (9) is equal to the toroidal part in (4). We will see that our techniques allow us to separate the poloidal and toroidal part of the geomagnetic field b in a natural way, which is an important feature for satellite missions like CHAMP. Since the poloidal and toroidal part of b are linked to the Mie scalars of the present currents via the pre–Maxwell equations, it is also possible to to recover these currents themselves.

6 Vector Spherical Harmonics

We now turn to the definition of basis systems suitable for the representations of vector fields. Let $l^2(\Omega)$ and $\mathcal{L}^2(\Omega)$, respectively, be the space of all square-integrable vector and scalar fields on the unit sphere Ω. $\{Y_{n,l}\}, n \in \mathbb{N}_0, l = 1, \ldots, 2n+1$, be a system of $\mathcal{L}^2(\Omega)$–orthonormal (scalar) spherical harmonics. As is well–known, every scalar field $F \in \mathcal{L}^2(\Omega)$ can be written as Fourier expansion

$$F = \sum_{n=0}^{\infty} \sum_{l=1}^{2n+1} F^\wedge(n,l)\, Y_{n,l}\,, \tag{11}$$

where the Fourier coefficients of F are given by $F^\wedge(n,l) = \int_\Omega F(\xi)\, Y_{n,l}(\xi)\, d\omega(\xi)$. We define for $i = 1,2,3$ a system of *vector spherical harmonics of type* i by $y_{n,l}^{(i)}(\xi) = \left(\mu_n^{(i)}\right)^{-\frac{1}{2}} o_\xi^{(i)} Y_{n,l}(\xi)$, with $\xi \in \Omega, n = 0_i, 0_i + 1, \ldots\ , \ l = 1, \ldots, 2n+1$, where $\mu_n^{(i)} = 1$ for $i = 1$, $\mu_n^{(i)} = n(n+1)$ for $i = 2,3$, $0_1 = 0$ and $0_2 = 0_3 = 1$. The factor $\mu_n^{(i)}$ is needed as a normalization factor, whereas the distinction of 0_1 and $0_2, 0_3$ is made since there exist constant radial fields but no constant tangential fields.

The system of all vector spherical harmonics of type 1,2 and 3 together is an orthonormal, complete system in the reference space $l^2(\Omega)$, such that every function $f \in l^2(\Omega)$ can be represented by its Fourier series

$$f = \sum_{i=1}^{3} \sum_{n=0_i}^{\infty} \sum_{l=1}^{2n+1} f_{n,l}^{(i)}\, y_{n,l}^{(i)}\,, \tag{12}$$

where the Fourier coefficients are given by

$$f_{n,l}^{(i)} = \left(f, y_{n,l}^{(i)}\right)_{l^2(\Omega)} = \int_\Omega f(\xi) \cdot y_{n,l}^{(i)}(\xi)\, d\omega(\xi)\,.$$

The separation of the basis system into vector spherical harmonics of type 1,2 and 3 is essential, since it permits us to recover a function according to the Helmholtz theorem and, hence, in accordance with the restrictions of the poloidal and toroidal part of the Mie representation to the sphere. However, the uncertainty priciple tells us that for the constructive part we should not use the vector harmonics, since these functions are suitable only for long–wavelength approximation. Moreover, from a computational point of view, any implementation of vector spherical harmonics requires the use of a particular coordinate system and leads to strong oscillations for higher degrees. Instead, we propose a different type of basis functions in the following section, namely (rotation–invariant) kernel functions. Nevertheless it should be kept in mind that $l^2(\Omega)$ is canonically split into three subspaces:

$$l^2_{(i)}(\Omega) = \overline{\bigoplus_{n=0_i}^{\infty} span_{l=1,\dots,2n+1} \{y_{n,l}^{(i)}\}}, \quad i = 1,2,3\ .$$

so that $l^2(\Omega)$ is the orthogonal direct sum of $l^2_{(1)}, l^2_{(2)}$ and $l^2_{(3)}$. For more details concerning scalar, vector and tensorial spherical harmonics the reader is referred to Freeden et al. (1998).

7 $l^2(\Omega)$-Kernel Functions

Consider now a special case of the Fourier series (12), where we choose $f_{n,l}^{(i)} = k^\wedge(n)\, Y_{n,l}(\eta)$ for $i \in \{1,2,3\}$ fixed, $\eta \in \Omega$ arbitrary but also fixed and where $\{k^\wedge(n)\}$, $n \in \mathbb{N}$ is a sequence of real numbers satisfying

$$\sum_{n=0_i}^{\infty} \frac{2n+1}{4\pi} |k^\wedge(n)|^2 < \infty\,.$$

Then we call the function

$$k^{(i)}(\xi,\eta) = \sum_{n=0_i}^{\infty} \sum_{l=1}^{2n+1} k^\wedge(n)\, Y_{n,l}(\eta)\, y_{n,l}^{(i)}(\xi) \tag{13}$$

an $l^2(\Omega)$-kernel function (briefly $l^2(\Omega)$-kernel). All of our following approximation techniques are based on kernels of the kind (13). Before we show how to do constructive approximation with these kernels we mention some properties of these kernels that are important from a numerical point of view. Firstly, $l^2(\Omega)$-kernels are easily computable. We find

$$\begin{aligned} k^{(i)}(\xi,\eta) &= \sum_{n=0_i}^{\infty} \sum_{l=1}^{2n+1} k^\wedge(n)\, Y_{n,l}(\eta)\, \left(\mu_n^{(i)}\right)^{-\frac{1}{2}}\, o_\xi^{(i)} Y_{n,l}(\xi) \\ &= o_\xi^{(i)} \sum_{n=0_i}^{\infty} \sum_{l=1}^{2n+1} k^\wedge(n)\, Y_{n,l}(\eta)\, \left(\mu_n^{(i)}\right)^{-\frac{1}{2}}\, Y_{n,l}(\xi) \\ &= o_\xi^{(i)} \sum_{n=0_i}^{\infty} \frac{2n+1}{4\pi} k^\wedge(n)\, \left(\mu_n^{(i)}\right)^{-\frac{1}{2}}\, P_n(\xi\cdot\eta), \end{aligned}$$

where P_n is the Legendre polynomial of degree n. In analogy to the Legendre polynomials we introduce Legendre vectors $p_n^{(i)}$ by

$$p_n^{(1)}(\xi,\eta) = \xi P_n(\xi\cdot\eta) \tag{14}$$
$$p_n^{(2)}(\xi,\eta) = (n(n+1))^{-1}\,(\eta-(\xi\cdot\eta)\,\xi)\;P_n'(\xi\cdot\eta) \tag{15}$$
$$p_n^{(3)}(\xi,\eta) = (n(n+1))^{-1}\,(\xi\wedge\eta)\,P_n'(\xi\cdot\eta)\,. \tag{16}$$

Using these vectors we finally arrive at

$$k^{(i)}(\xi,\eta) = \sum_{n=0_i}^{\infty}\frac{2n+1}{4\pi}\,k^{\wedge}(n)\,\left(\mu_n^{(i)}\right)^{\frac{1}{2}}\,p_n^{(i)}(\xi,\eta)\,. \tag{17}$$

Hence, in order to evaluate the kernel (13) we have to evaluate the series (17). For series in terms of (14), (15) and (16) there exist fast and stable one-dimensional recursive algorithms, (see e.g. Deufelhard (1975)). Furthermore, from (17), we conclude that these kernels, although defined via vector spherical harmonics, do not require any particular coordinate system such that the poles are no exceptional points. Moreover, the uncertainty principle (cf. Freeden (1999), Beth (1999)) informs us that the varieties of the intensity of space/frequency localization on the sphere Ω can also be illustrated formally by considering the sequence $\{k^{\wedge}(n)\}$ of the kernel functions. By choosing $k^{\wedge}(n)=\delta_{n,l}$ we formally obtain a vector spherical harmonic of degree l, i.e. a vector field with ideal frequency localization, but no space localization. On the other hand, if we set $k^{\wedge}(n)=1$ for all n we obtain the kernel which is the Dirac functional in $l^2_{(i)}(\Omega)$. Bandlimited kernels satisfy $k^{\wedge}(n)=0$ for all $n>N$ for some integer N. Non-bandlimited kernels satisfy $k^{\wedge}(n)\neq 0$ for an infinite number of integers n. Assuming the property $\lim_{n\to\infty}k^{\wedge}(n)=0$ it follows from the uncertainty principle that the slower the sequence $\{k^{\wedge}(n)\}$ converges to zero, the lower is the frequency localization, and the higher is the space localization.

8 Convolutions

One of our main scopes is the recovery of vector fields, in particular the geomagnetic field, from given discrete vectorial data. For our $l^2(\Omega)$-kernel based methods we need two types of convolutions. Our treatment will be brief (for details confer Bayer et al. (1998), a different convolution approach is indicated in Freeden et al. (1998) which will not be discussed here):

(i) the *convolution of an $l^2(\Omega)$-kernel $k^{(i)}$ against a vector-valued function $f\in l^2(\Omega)$* is defined by

$$\begin{aligned}(k^{(i)}*f)(\xi) &= \int_{\Omega}k^{(i)}(\eta,\xi)\cdot f(\eta)\;d\omega(\eta) \\ &= \sum_{n=0_i}^{\infty}\sum_{l=1}^{2n+1}k^{\wedge}(n)\,f_{n,l}^{(i)}\,Y_{n,l}(\xi),\qquad \xi\in\Omega\end{aligned} \tag{18}$$

(ii) the *convolution of an $l^2(\Omega)$-kernel $k^{(i)}$ against a scalar-valued function $F \in \mathcal{L}^2(\Omega)$* is defined as

$$\begin{aligned}(k^{(i)} \star F)(\xi) &= \int_\Omega k^{(i)}(\xi,\eta)\, F(\eta)\; d\omega(\eta) \\ &= \sum_{n=0_i}^{\infty} \sum_{l=1}^{2n+1} k^\wedge(n)\, F^\wedge(n,l)\, y_{n,l}^{(i)}(\xi), \qquad \xi \in \Omega\,.\end{aligned} \tag{19}$$

Let now $h^{(i)}$ and $k^{(i)}$ be two $l^2(\Omega)$-kernels. Combining (i) and (ii) we obtain the *convolution of $h^{(i)} \star k^{(i)}$ against a vector-valued function $f \in l^2(\Omega)$* defined by

$$(h^{(i)} \star k^{(i)} * f)(\xi) = \sum_{n=0_i}^{\infty} \sum_{l=1}^{2n+1} k^\wedge(n)\, h^\wedge(n)\, f_{n,l}^{(i)}\, y_{n,l}^{(i)}(\xi) \qquad \xi \in \Omega. \tag{20}$$

As we recognize, Eq. (20) yields a filtered version of $f^{(i)}$. More explicitly, the Fourier coefficients are filtered by the factor $k^\wedge(n)\, h^\wedge(n)$ for each $n = 0_i, 0_i + 1, \ldots$. This observation leads to the notion of a multiresolution analysis (MRA) in terms of scaling functions and wavelets.

9 The Scaling Function

We turn now to the constructive part of this paper. Most of the underlying ideas can be found in Freeden and Windheuser (1997) and Freeden and Schreiner (1998), for more applications to vectorial problems the reader should consult Freeden et al. (1998) and Bayer et al. (1998). Let $\varphi_0^{(i)} : [0,\infty) \to \mathbb{R}$, $i = 1,2,3$ be three functions satisfying the following conditions:

(i) $\varphi_0^{(i)}$ is monotonically decreasing,

(ii) $\varphi_0^{(i)}$ is piecewise continuous in $(0,\infty)$ and continuous at 0,

(iii) $\varphi_0^{(i)}(0) = 1$,

(iv) $\sum_{n=0_i}^{\infty} \frac{2n+1}{4\pi} |\varphi_0^{(i)}(n)|^2 < \infty$.

Then $\varphi_0^{(i)}$ is called the *generator* of the scale discrete scaling function of type i, which is defined as

$$\Phi_0^{(i)}(\xi,\eta) = \sum_{n=0_i}^{\infty} \sum_{l=1}^{2n+1} \varphi_0^{(i)}(n)\, y_{n,l}^{(i)}(\xi)\, Y_{n,l}(\eta), \qquad (\xi,\eta) \in \Omega^2,\ i = 1,2,3\,. \tag{21}$$

The dilates of the generator of the scaling functions are defined by

$$D_j \varphi_0^{(i)}(x) = \varphi_j^{(i)}(x) = \varphi_0^{(i)}(2^{-j}x),\ i = 1,2,3,$$

and accordingly we set the dilated scaling function

$$D_j\Phi_0^{(i)}(\xi,\eta) = \Phi_j^{(i)}(\xi,\eta) = \sum_{n=0_i}^{\infty}\sum_{l=1}^{2n+1} \varphi_j^{(i)}(n)\, y_{n,l}^{(i)}(\xi)\, Y_{n,l}(\eta), \quad (\xi,\eta)\in\Omega^2, \qquad j\in\mathbb{Z}\,. \tag{22}$$

Eq. (22) is well defined, since we have

$$\sum_{n=0_i}^{\infty} \frac{2n+1}{4\pi}\,|\varphi_j^{(i)}(n)|^2 < \infty\,,$$

provided that condition (iv) imposed on $\varphi_0^{(i)}$ holds (for details see Freeden and Schreiner (1998)).

We turn now to a central result of our method: Let $f = f^{(1)} + f^{(2)} + f^{(3)} \in l^2(\Omega)$ and let $\Phi_0^{(i)}$ be a scale discrete scaling function as in (21). Then $f^{(i)}$ can be approximated by filtered versions of itself as follows:

$$\lim_{J\to\infty} \|\Phi_J^{(i)} \star \Phi_J^{(i)} * f - f^{(i)}\|_{l^2(\Omega)} = 0, \qquad i = 1,2,3\,. \tag{23}$$

This is why the sequence $\{\Phi_J^{(i)}\}$, $J\in\mathbb{N}$ is also called an *approximate convolution identity* in $l^2_{(i)}\Omega$, $i=1,2,3$. Eq. (23) means that for each $J\in\mathbb{N}$ we get an approximation $\Phi_J^{(i)} \star \Phi_J^{(i)} * f$ of $f^{(i)}$, and that these approximations become arbitrarily exact (in the $l^2(\Omega)$-sense) as $J\to\infty$. Now we pack all possible J-level approximations together in so-called scale spaces $\mathcal{V}_J^{(i)}$. More precisely, for every $f\in l^2(\Omega)$ we define the operator $P_J^{(i)}$ by $P_J^{(i)}(f) = \Phi_J^{(i)} \star \Phi_J^{(i)} * f$, and accordingly we set $\mathcal{V}_J^{(i)} = \{P_J^{(i)}(f) \mid f\in l^2(\Omega)\}$, for $i=1,2,3$.

The dilation operator D_j is constructed in such a way that the corresponding scale spaces are nested, (cf. Bayer et al. (1998)) i.e. they satisfy

$$\mathcal{V}_0^{(i)} \subset \ldots \subset \mathcal{V}_l^{(i)} \subset \mathcal{V}_{l+1}^{(i)} \subset \ldots \subset l^2_{(i)}(\Omega), \qquad i=1,2,3,$$

In other words, a space corresponding to some resolution contains all the information about the space at a lower resolution. Moreover, we have

$$\overline{\bigcup_{j=0}^{\infty}\mathcal{V}_j^{(i)}}^{\|\cdot\|_{l^2(\Omega)}} = l^2_{(i)}(\Omega), \qquad i=1,2,3,$$

which is just another way of stating Eq. (23). In short, for every level $J\in\mathbb{N}$ we obtain an approximation of $f^{(i)}$ that improves with increasing J and we speak of $P_J^{(i)}(f)$ as a *single scale expansion* of $f^{(i)}$. The multiresolution is based on filtering in the frequency space. Several construction principles can be found in the literature (for details see Freeden et al. (1998) and the references therein).

10 Wavelets

Next we introduce (scale discrete) wavelets. Although the principle of a multiresolution analysis by means of the scaling function yields an approximation sequence of increasing accuracy it is

desirable to have a more structured approach that permits statements about the 'gaps', i.e. the detail information between two successive scale spaces. This structure is obtained by the use of wavelets. Since the construction of such wavelets is extensively treated in the literature (for a summary of the material see Freeden et al. (1998)), we keep our treatment brief. The idea is to split a J-level approximation into smaller building blocks. In our context this is once more done in the frequency space. Let, therefore, $\Phi_0^{(i)}$ be a scale discrete scaling function as before. Moreover, let $\psi_0^{(i)}, \tilde{\psi}_0^{(i)} : [0,\infty) \to \mathbb{R}$, $i = 1,2,3$ satisfy the following conditions:

(i) $\psi_0^{(i)}, \tilde{\psi}_0^{(i)}$ are piecewise continuous in $[0,\infty)$,

(ii) $\sum\limits_{n=0_i}^{\infty} \frac{2n+1}{4\pi} |\psi_0^{(i)}(n)|^2 < \infty$, $\sum\limits_{n=0_i}^{\infty} \frac{2n+1}{4\pi} |\tilde{\psi}_0^{(i)}(n)|^2 < \infty$,

(iii) $\tilde{\psi}_0^{(i)}(x)\psi_0^{(i)}(x) = \left(\varphi_0^{(i)}(\frac{x}{2})\right)^2 - \left(\varphi_0^{(i)}(x)\right)^2$, $x \in [0,\infty)$.

Then $\psi_0^{(i)}, \tilde{\psi}_0^{(i)}$ define the scale discrete mother wavelet of type i $\Psi_0^{(i)}$ and its dual $\tilde{\Psi}_0^{(i)}$ by

$$\Psi_0^{(i)}(\xi,\eta) = \sum_{n=0}^{\infty} \sum_{l=1}^{2n+1} \psi_0^{(i)}(n)\, y_{n,l}^{(i)}(\xi)\, Y_{n,l}(\eta), \qquad (\xi,\eta) \in \Omega^2, \tag{24}$$

$$\tilde{\Psi}_0^{(i)}(\xi,\eta) = \sum_{n=0}^{\infty} \sum_{l=1}^{2n+1} \tilde{\psi}_0^{(i)}(n)\, y_{n,l}^{(i)}(\xi)\, Y_{n,l}(\eta), \qquad (\xi,\eta) \in \Omega^2. \tag{25}$$

As before the dilation operator D_j can be applied to the mother wavelet and its dual, such that we obtain a dilated version at all levels $J \in \mathbb{N}$:

$$D_j\Psi_0^{(i)}(\xi,\eta) = \Psi_j^{(i)}(\xi,\eta) = \sum_{n=0}^{\infty} \sum_{l=1}^{2n+1} \psi_j^{(i)}(n)\, y_{n,l}^{(i)}(\xi)\, Y_{n,l}(\eta), \qquad \xi,\eta \in \Omega, \tag{26}$$

$$D_j\tilde{\Psi}_0^{(i)}(\xi,\eta) = \tilde{\Psi}_j^{(i)}(\xi,\eta) = \sum_{n=0}^{\infty} \sum_{l=1}^{2n+1} \tilde{\psi}_j^{(i)}(n)\, y_{n,l}^{(i)}(\xi)\, Y_{n,l}(\eta), \qquad \xi,\eta \in \Omega. \tag{27}$$

To have a notation consistent with existing wavelet techniques we introduce the rotation operator (that replaces the shift operator in standard Euclidean theory of wavelets). Performing the rotation after the dilation we can write wavelets at all scales and positions as dilated and rotated versions of one mother wavelet by

$$\Psi_j^{(i)}(\xi,\eta) = \Psi_{j;\xi}^{(i)}(\eta) = (R_\xi D_j \Psi_0^{(i)})(\cdot,\eta), \qquad (\xi,\eta) \in \Omega^2,$$
$$\tilde{\Psi}_j^{(i)}(\xi,\eta) = \tilde{\Psi}_{j;\xi}(\eta) = (R_\xi D_j \tilde{\Psi}_0^{(i)})(\cdot,\eta), \qquad (\xi,\eta) \in \Omega^2\,.$$

We are now in a position to define the *spherical vector wavelet transform* of a vector field by

$$(WT)_{\Psi_0^{(i)}}(f)(j;\eta) = (\Psi_j^{(i)} * f)(\eta) = \int_\Omega \Psi_j^{(i)}(\xi,\eta) \cdot f(\xi)\, d\omega(\xi) \tag{28}$$

for $j \in \mathbb{N}, \eta \in \Omega$ and $i = 1, 2, 3$.

The central result for the application of wavelets is the following inversion formula, that tells us how to reconstruct a vector field from its wavelet transform: Let therefore $\Phi_0^{(i)}, \Psi_0^{(i)}, \tilde{\Psi}_0^{(i)}$ be as before. Then, for any $f = f^{(1)} + f^{(2)} + f^{(3)} \in l^2(\Omega)$, the *reconstruction formula* reads as follows

$$\begin{aligned} f^{(i)} &= \Phi_0^{(i)} \star \Phi_0^{(i)} * f + \sum_{j=0}^{\infty} \int_\Omega (WT)_{\Psi_0^{(i)}}(f)(j;\eta)\ \tilde{\Psi}_j^{(i)}(\cdot,\eta)\, d\omega(\eta) \qquad (29) \\ &= \Phi_0^{(i)} \star \Phi_0^{(i)} * f^{(i)} + \sum_{j=0}^{\infty} \tilde{\Psi}_j^{(i)} \star \Psi_j^{(i)} * f\,. \end{aligned}$$

The single scale expansion in terms of scaling functions known from Chapter 9 can now be written as a *multiscale expansion* by

$$\Phi_J^{(i)} \star \Phi_J^{(i)} * f = \Phi_0^{(i)} \star \Phi_0^{(i)} * f + \sum_{j=0}^{J-1} \tilde{\Psi}_j^{(i)} \star \Psi_j^{(i)} * f\ . \qquad (30)$$

The scaling function at any scale can be replaced by the scaling function at a lower scale and the corresponding wavelets at all intermediate scales. This is the reason why we speak of wavelets as "building blocks". Instead of computing a new single scale expansion to improve our approximation we only add the information that is really "new", i.e. the detail information between two subsequent scale spaces. This new information is contained in the wavelet transform. Analogously to the scale spaces $\mathcal{V}_j^{(i)}$ and the corresponding operators $P_j^{(i)}$ we now define detail spaces $\mathcal{W}_j^{(i)}$ and operators $R_j^{(i)}$ by

$$R_j^{(i)}(f) = \tilde{\Psi}_j^{(i)} \star \Psi_j^{(i)} * f, \quad f \in l^2(\Omega)\ ,$$

and $\mathcal{W}_j^{(i)} = \{R_j^{(i)}(f) \,|\, f \in l^2(\Omega)\}$. The scale and detail spaces allow similar statements as in (30), i.e. we can display a scale space as the sum of a scale space at a lower level and all intermediate detail spaces:

$$\mathcal{V}_J^{(i)} = \mathcal{V}_M^{(i)} + \sum_{j=M}^{J-1} \mathcal{W}_j^{(i)}\ , \quad M < J\,. \qquad (31)$$

We mention that the sum in (31) is in general neither direct nor orthogonal. It can be made orthogonal, though, if we wish to construct so-called Shannon wavelets.

11 Examples

We give now a more concrete description of our mother wavelet and its dual. We restrict ourselves to so-called P-wavelets here, but other strategies exist and have been implemented, such as so-called M-, D- or S-wavelets (cf. Freeden and Windheuser (1997), Freeden (1999)).

Let $\varphi_0^{(i)}$ be the generator of a scale discrete scaling function (21) for $i \in \{1,2,3\}$. Then we choose

$$\psi_0^{(i)}(x) = \sqrt{\left(\varphi_1^{(i)}(x)\right)^2 - \left(\varphi_0^{(i)}(x)\right)^2},\ x \in [0,\infty), \tag{32}$$

$$\tilde{\psi}_0^{(i)}(x) = \sqrt{\left(\varphi_1^{(i)}(x)\right)^2 - \left(\varphi_0^{(i)}(x)\right)^2},\ x \in [0,\infty)\,. \tag{33}$$

The P-wavelet and its dual coincide, and it is obvious that the conditions (i) – (iii) in Section 10 are fulfilled. We distinguish two large classes of wavelets and scaling functions, namely bandlimited and non-bandlimited kernels. We already mentioned that bandlimited means that the series (24) and (25) are finite, i.e. the generators $\psi_0^{(i)}$, $\tilde{\psi}_0^{(i)}$ have compact support. Without loss of generality we require that this finite support is the interval $[0,1]$. As examples we give the (non-bandlimited) Abel-Poisson P-wavelet and the bandlimited Shannon and CUP P-wavelets. Note that we chose to plot the *tangential* kernels ($i = 2,3$) only. The $i = 3$ component is the one that can be identified with the toroidal part of the geomagnetic field. It is clearly visible that the significant support of the wavelets decreases with increasing scale, which is a feature typical for wavelets. This property allows a zooming-in on small-scale features of the observed field (e.g. the geomagnetic field).

The Abel-Poisson wavelet: Here we have $\varphi_0^{(i)}(x) = r^x$ with some fixed $r \in (0,1)$ and the generators of the wavelet and its dual are computed according to (32) and (33). Figure 1 shows the Abel-Poisson wavelets at scales 2 and 3, where we chose $r = 1/e$.

The Shannon wavelet: This is the simplest conceivable choice of bandlimited wavelets: We set

$$\varphi_0^{(i)}(x) = \begin{cases} 1, & x \in [0,1) \\ 0, & \text{else} \end{cases}$$

Because of the sharp cutting in the frequency domain we obtain orthogonal detail spaces with no redundance. However, this leads to strong oscillations in the space domain, as can be seen in Figure 2, which may cause serious difficulties for computational purposes.

The CUP–wavelet: We look for a way to preserve the band-limited character of the wavelets such that the oscillations are at least reduced in contrast to the Shannon wavelet. One possibility is to smooth the representation in the frequency space. We choose

$$\varphi_0^{(i)}(x) = \begin{cases} (1-x)^2(1+2x) & , \quad x \in [0,1) \\ 0 & , \quad x \in [1,\infty). \end{cases}$$

In doing so we give up the orthogonality of the detail spaces, but we can still work with band-limited integration techniques and the oscillations are widely supressed, (see Figure 3). The CUP wavelets proved to be a good compromise for the numerical treatment of MAGSAT data, as the examples in the following section show. For more details on band-limited integration see for example Bayer et al. (1998), Freeden (1999).

In all three cases we can clearly make out the character of the kernels as surface-divergence-free and surface-curl-free vector fields. For the applications this means that the tangential part of a vector field can be decomposed into its poloidal and toroidal component. One more remark concerning Figures 1, 2 and 3. Looking closely we observe that these tangential vectorial

functions do *not* have their maximal absolute value at $\xi = \eta$ but that they are zero at this position. This is contrary to the kernel with $i = 1$ (i.e. the kernel corresponding to the normal field) or the kernels we know from scalar theory. The reason is the structure of the Legendre vectors (15) and (16) used in (17). The *scalar* part, i.e. the series in terms of the first derivatives of the Legendre polynomials *does* have its maximum at $\xi = \eta$. However, the *vectorial* part in (15) and (16) is zero there. Thus, the maximum lies somewhere outside the position $\xi = \eta$.

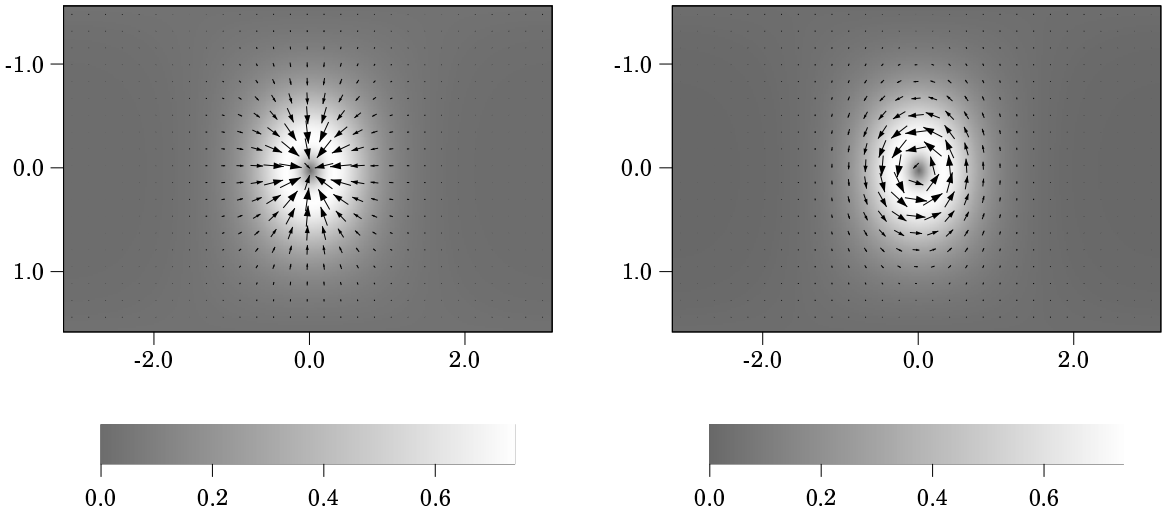

scale $j = 2$: $i = 2$ (curl-free part) left, $i = 3$ (divergence-free part) right

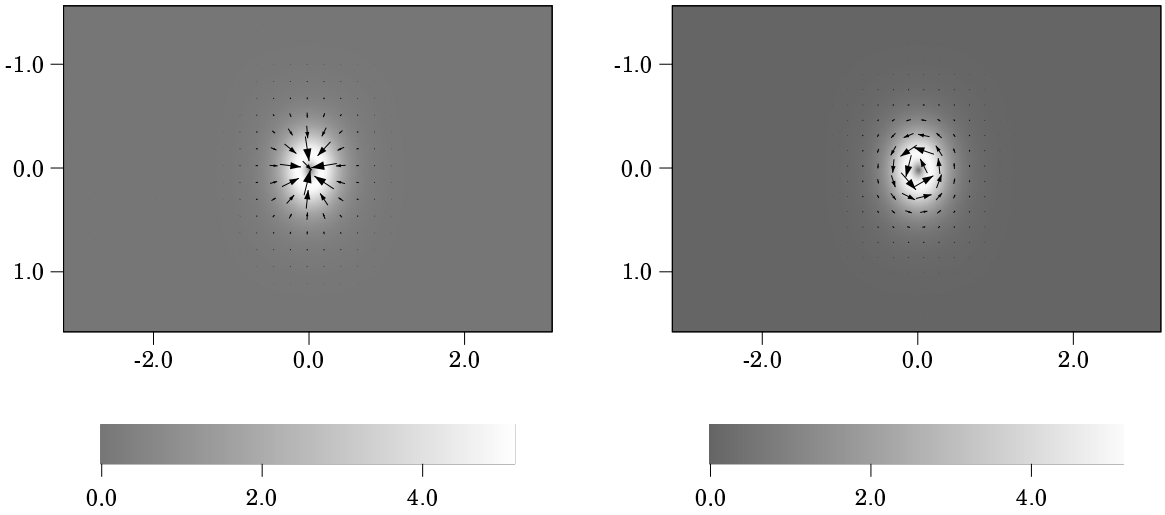

scale $j = 3$: $i = 2$ (curl-free part) left, $i = 3$ (divergence-free part) right

Figure 1: Abel-Poisson P-wavelet

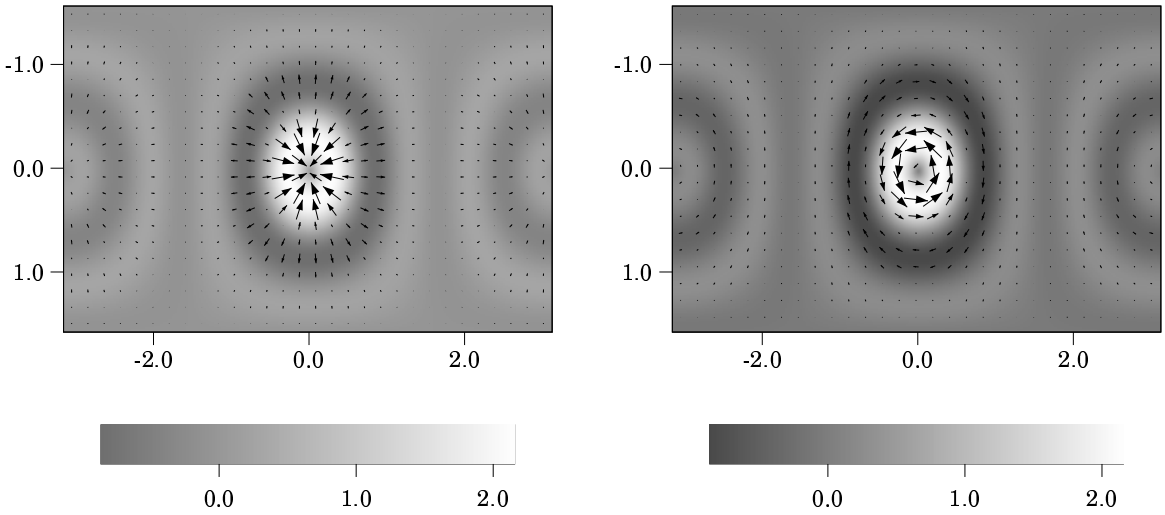

scale $j = 2$: $i = 2$ (curl-free part) left, $i = 3$ (divergence-free part) right

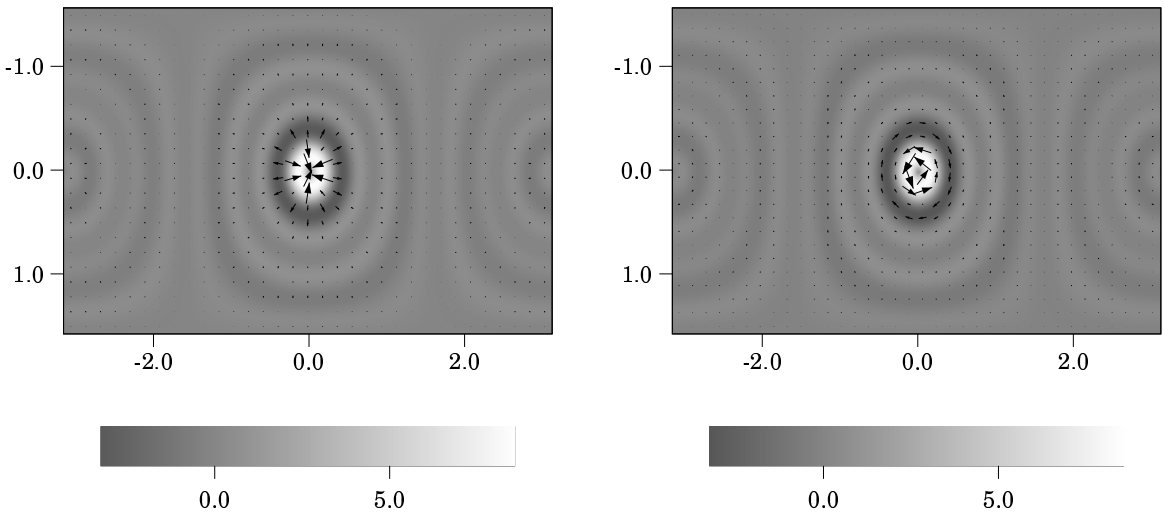

scale $j = 3$: $i = 2$ (curl-free part) left, $i = 3$ (divergence-free part) right

Figure 2: Shannon P-wavelet

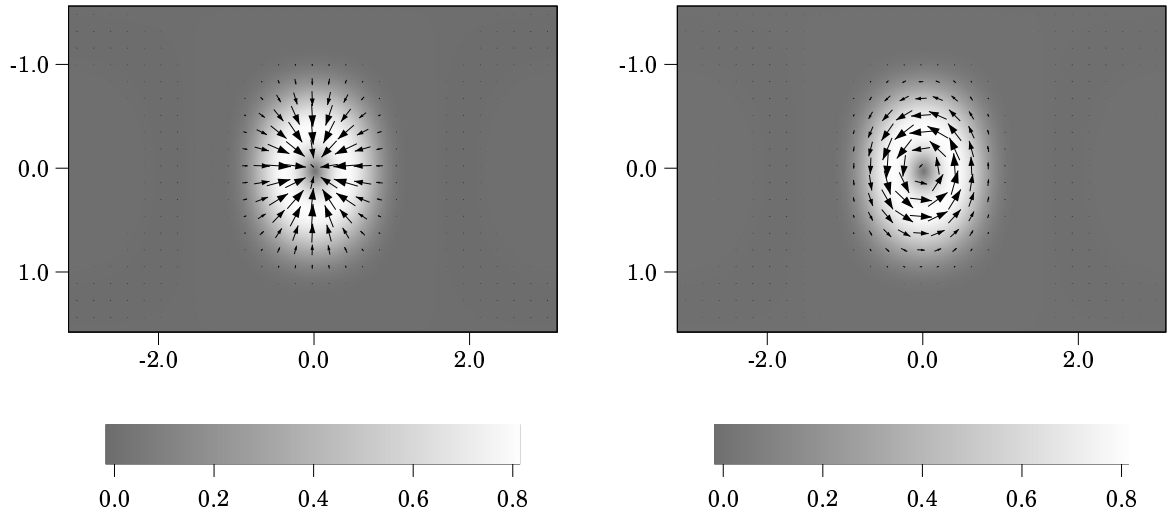

scale $j = 2$: $i = 2$ (curl-free part) left, $i = 3$ (divergence-free part) right

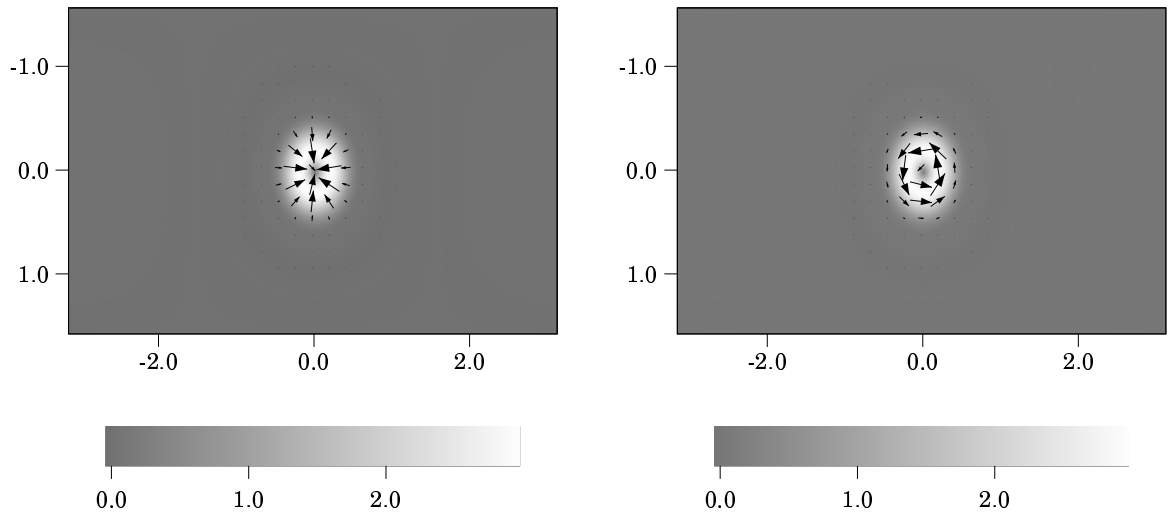

scale $j = 3$: $i = 2$ (curl-free part) left, $i = 3$ (divergence-free part) right

Figure 3: CUP P-wavelet

12 An Application of CUP-Wavelets to MAGSAT Data

In this section we analyse a data set derived from vectorial MAGSAT morning data that has been contributed by Nils Olsen of the Danish Space Research Institute. The measurements are averaged on a longitude-latitude grid with ($\Delta\varphi = 4^o, \Delta\vartheta = 2^o$) in geomagnetic coordinates. The radial variations of the MAGSAT satellite have been neglected in the dataset and, therefore, prior to the averaging process, the GSFC(12/83) reference potential model has been subtracted

to avoid spurious effects. The data used results from one month of measurements, centered at March 21, 1980.

In what follows we decompose and reconstruct the given data by CUP P-wavelets (see Chapter 10). In particular we plot the component pointing to the geographic east direction, i.e. in geophysical language the Y-component of the toroidal part at different scales (see Figures 4 and 5). Note that the toroidal part is obtained by wavelets of type $i = 3$. The detail approximations in Figures 4, 5 show large magnetic effects in the polar regions and a band-like magnetic structure in the close vicinity of the equatorial line. The first is due to large field aligned currents in high latitudes, while the latter is due to the radial component of the equatorial electrojet (EEJ). Hence, both magnetic effects are caused by ionospheric and magnetospheric current systems and can therefore *not* be modelled correctly by a Gaussian gradient field.

The multiscale analysis shows that these magnetic features are of small to medium scale. At scales $j = 0, 1, 2$ the visible structures are spatially large and none of the above mentioned effects can be recognized, while from scale $j = 3$ up to scale $j = 6$ the EEJ as well as the polar contributions are predominant.

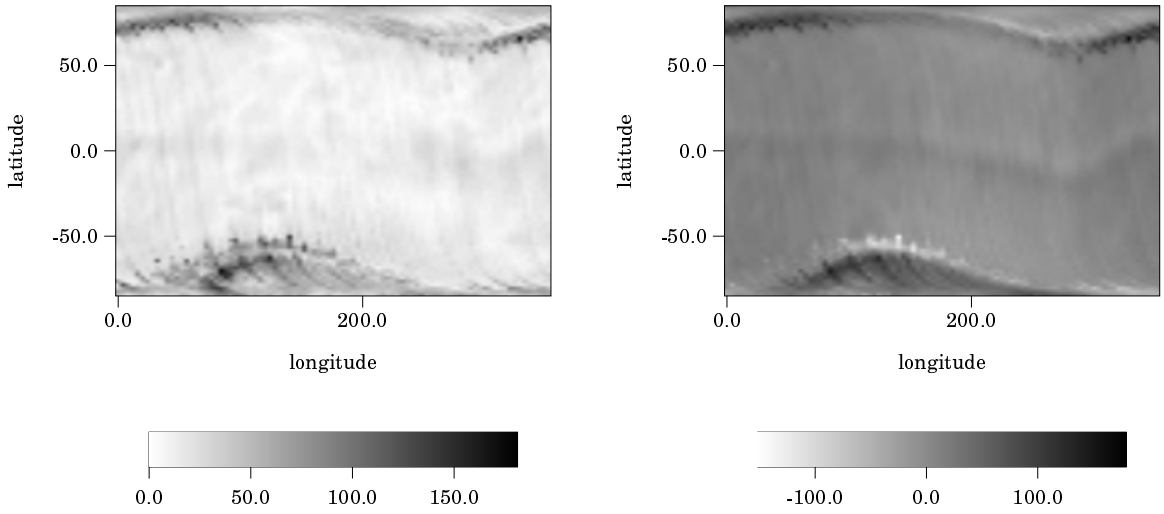

Input data (MAGSAT): intensity left, geophysical Y-component (East) right [nT]

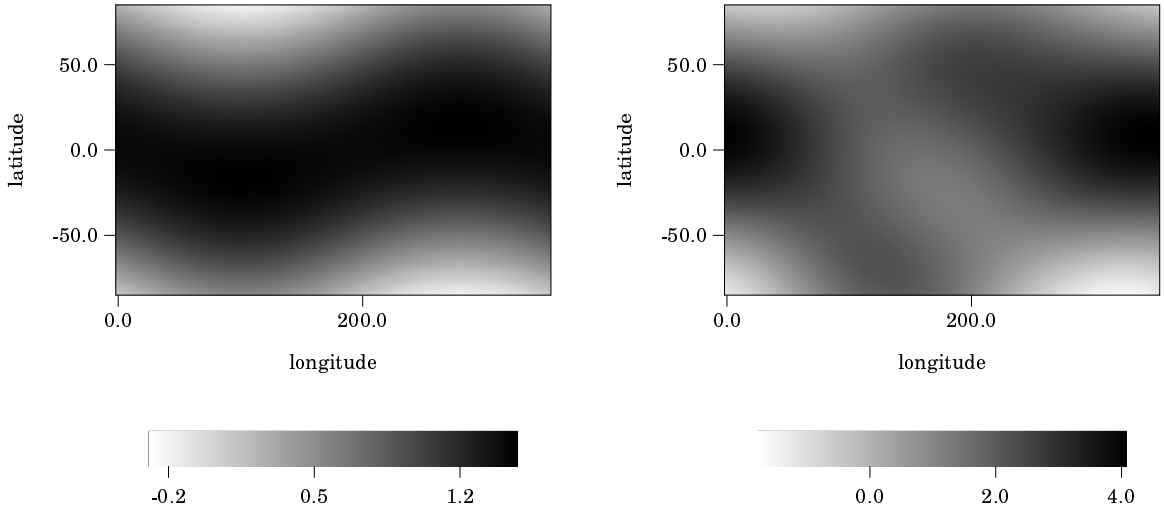

Y-component detail approximation of toroidal part: $j = 0$ left, $j = 1$ right [nT]

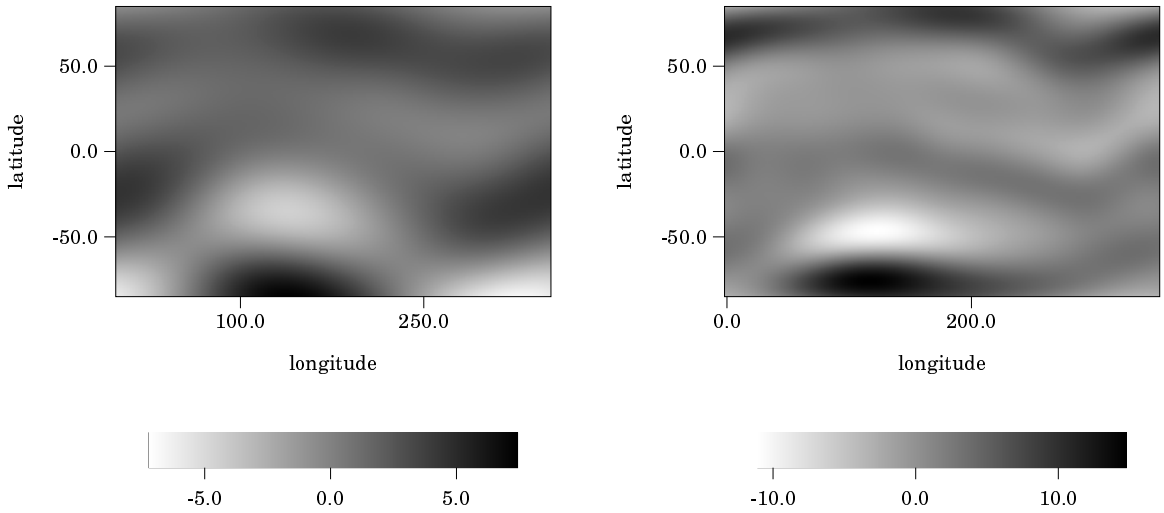

Y-component detail approximation of toroidal part: $j = 2$ left, $j = 3$ right [nT]

Figure 4: Input data and CUP-Wavelet approximation of the toroidal part at different scales

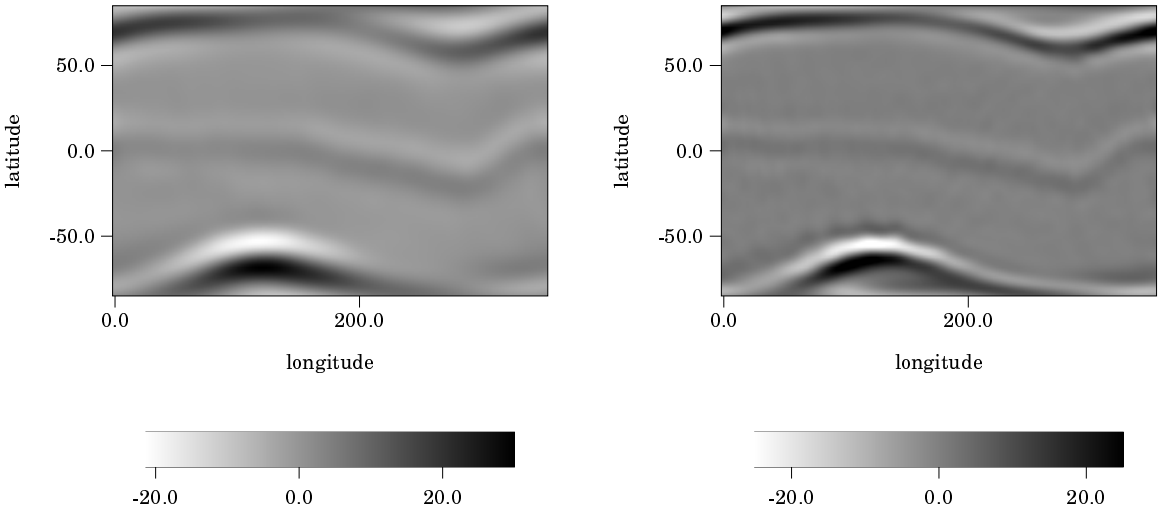

Y-component detail approximation of toroidal part: $j = 4$ left, $j = 5$ right [nT]

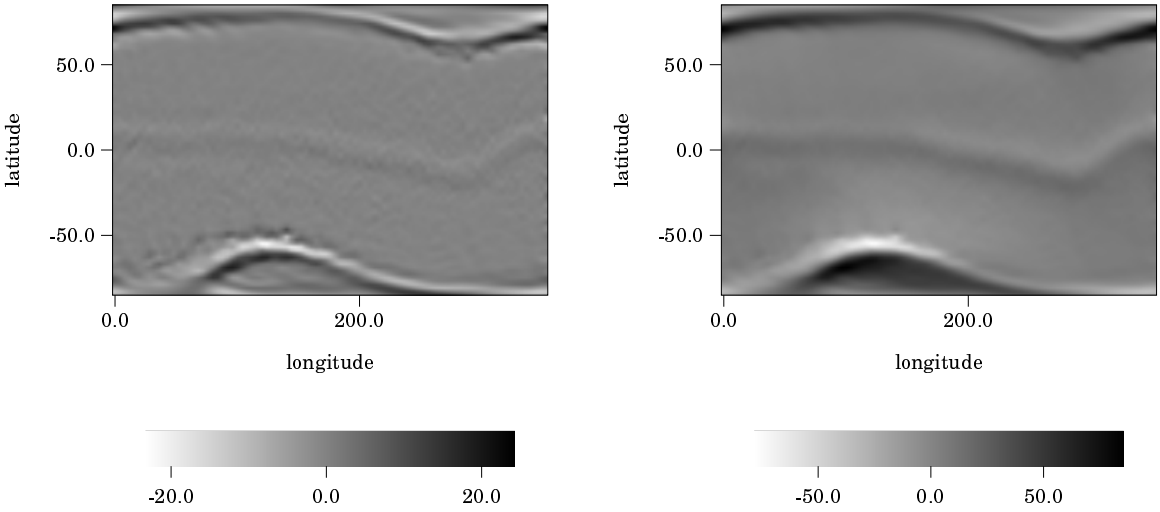

Y-comp. detail approximation, toroidal part: $j = 6$ left, $j = 0, \ldots, 6$ added up right [nT]

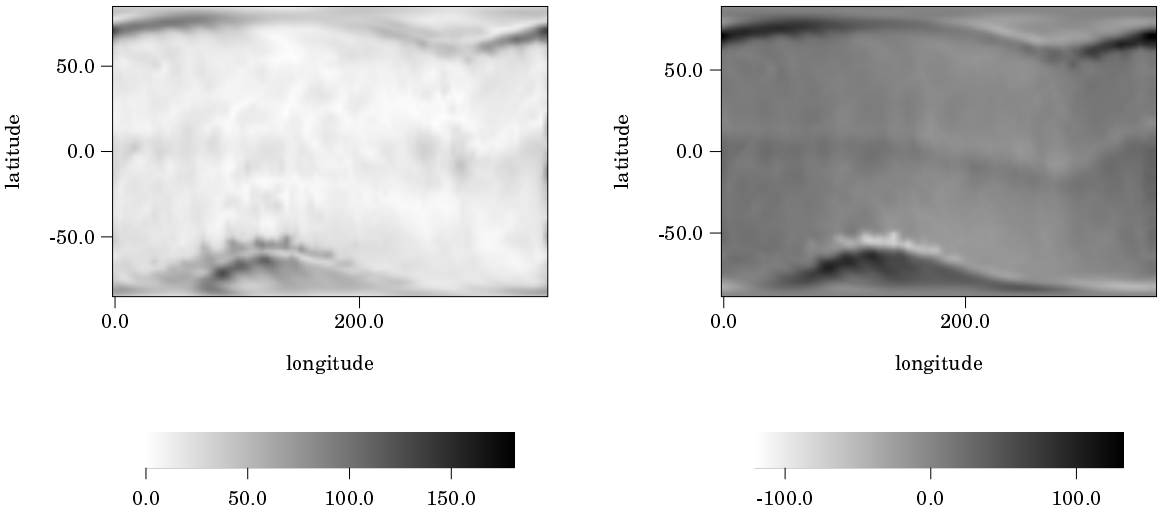

Total reconstructed field (poloidal and toroidal): intensity left, Y-component right [nT]

Figure 5: CUP-Wavelet approximation of the toroidal part at different scales and total reconstruction

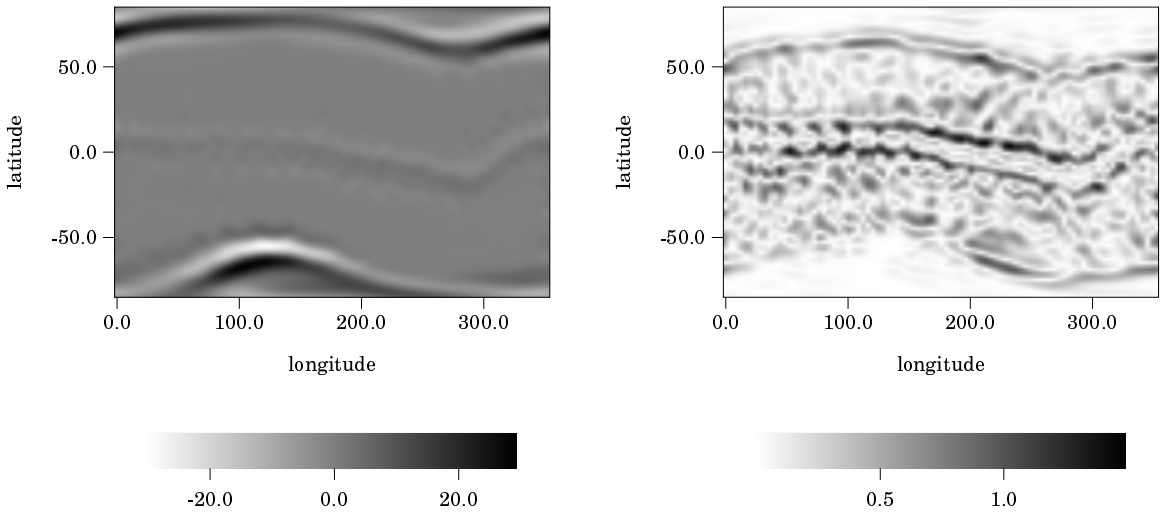

Figure 6: Reconstruction with compressed coefficient set at $j = 5$ left, corresponding error right [nT]

Finally we demonstrate the data compression capability of wavelets. Since wavelets localize more and more in space domain, for higher scales only very few wavelet coefficients are significantly different from zero. The idea is therefore to discard most coefficients and to keep only those greater than a prescribed threshold in order to save computing time and storage capacity. As an example we consider the CUP wavelet as above at scale $j = 5$. The threshold has been set to 3 nT which results in a compression rate of 62.06 per cent. The corresponding reconstruction and error plot is shown in Figure 6. The maximal error was 1.4 nT, the mean quadratic error was 0.24 nT. More numerical tests concerning multiscale computation of the geomagnetic field has been performed in Maier (1999).

Conclusion

In theory, the Mie representation of the magnetic field can be reconstructed from its Fourier transform i.e. the 'amplitude spectrum' in terms of *vector* harmonics representing the poloidal and toroidal contribution, but the Fourier transform contains information about the frequencies of the field over all positions instead of showing how the frequencies vary in space. In future research, Fourier expansions in terms of vector harmonics will therefore not be the most natural and useful way of representing the magnetic field. In fact, we have to think of the magnetic field as a signal in which the amplitude spectrum evolves over space in a significant way. We imagine that at each point in space the field refers to a certain combination of frequencies, and that in dependence on the location of sources the contribution to the frequencies and therefore the frequencies themselves are spatially changing. This space–evolution of the frequencies is not reflected in the Fourier transform in terms of non–space localizing vector harmonics, at least not directly. A method of achieving a space–dependent frequency analysis in magnetic field modelling is the wavelet approximation as presented in this paper. The wavelet transform

acts as a space and frequency localization operator. Numerical work can be efficiently executed by a multiresolution analysis, i.e. a completely recursive method which is therefore ideal for computation.

References

[1] Backus, G. (1986) Poloidal and Toroidal Fields in Geomagnetic Field Modelling. Rev. Geophys.,**24**, 75–109.

[2] Backus, G., Parker, R., Constable, C. (1996) Foundations of Geomagnetism. Cambridge University Press, Cambridge.

[3] Bayer, M., Beth, S., Freeden, W. (1998) Geophysical Field Modelling by Multiresolution Analysis. Acta Geod. Geoph. Hung., **33**, 289-319.

[4] Beth, S. (1999) Spherical Vector Wavelets: Theoretical and Numerical Aspects (With an Application to Physical Geodesy). PhD Thesis, University of Kaiserslautern, Geomathematics Group (in preparation).

[5] Cain, C.J., Schmitz, D.R., Muth, L. (1984) Small-Scale Features in the Earth's Magnetic Field Observed by MAGSAT. J. Geophy. Res., **89**, 1070–1076.

[6] Deuflhard, P. (1975) On Algorithms for the Summation of Certain Special Functions. Computing, **17**, 37-48.

[7] Donovan, E.F. (1993) Modeling the magnetic effects of field–aligned currents. J. Geophys. Res., **98**, 529–543.

[8] Driscoll, J.R., Healy, R.M. (1994) Computing Fourier Transforms and Convolutions on the 2–Sphere. Adv. Appl. Math., **15**, 202-250.

[9] Engels, U., Olsen, N. (1998) Computation of Magnetic Fields Within Sources Regions of Ionospheric and Magnetospheric Currents. J. Atmosph. and Solar–Terrestrial Physics, **60**, 1585–1592.

[10] Freeden, W. (1981) On Approximation by Harmonic Splines. Manuscr. Geod., **6**, 193–244.

[11] Freeden, W., Gervens, T. (1991) Vector Spherical Spline Interpolation (Basic Theory and Computational Aspects). Math. Meth. in the Appl. Sci., **16**, 151–183.

[12] Freeden, W. (1998) The Uncertainty Principle and Its Role in Physical Geodesy. Progress in Geodetic Science (at GW98), 225–227, Shaker-Verlag, Aachen.

[13] Freeden, W. (1999) Multicale Modelling of Spaceborne Geodata. Teubner–Verlag, Stuttgart, Leipzig.

[14] Freeden, W., Gervens, T., Schreiner, M. (1998) Constructive Approximation on the Sphere (With Applications to Geomathematics). Oxford Science Publications, Clarendon Press.

[15] Freeden, W., Glockner, O., Schreiner, M. (1999) Spherical Panel Clustering and Its Numerical Aspects. J. Geod., **72**, 586–599.

[16] Freeden, W., Schreiner, M. (1998) Orthogonal and Nonorthogonal Multiresolution Analysis, Scale Discrete and Exact Fully Discrete Wavelet Transform o the Sphere. Constr. Appr., **14**, 493–515.

[17] Freeden, W., Windheuser, U. (1997) Combined Spherical Harmonic and Wavelet Expansion — A Future Concept in Earth's Gravitational Potential Determination. Appl. Comput. Harm. Anal. (ACHA), **4**, 1-37.

[18] Gauss, C.F. (1836) Allgemeine Theorie des Erdmagnetismus. Resultate aus den Beobachtungen des magnetischen Vereins im Jahre 1838 (English translation: Gauss, C.F. (1838)) General Theory of Terrestrial Magnetism. In. R. Taylor (ed.) Scientific Memoirs selected from the Transactions of Foreing Academies of Science and Learned Societies and From Foreign Journals, **2**, 184-251, 1841).

[19] Iijima, T. Potemra, A., (1978) Large–scale Characteristics of Field–aligned Currents Associated With Substorms. J. Geophys. Res. **83**, 599–615.

[21] Kisabeth, J.L. (1979) On Calculating Magnetic and Vector Potential Field Due to Large–Scale Magnetospheric Currents Systems and Induced Currents in an Infinitely Conducting Earth. In Quantitative Modelling Magnetospheric Processes, W. P. Olsen (ed.), American Geophysical Union.

[22] Kosik, J.C. (1984) Quantitative Magnetospheric Field Modelling with Toroidal and Poloidal Vector Fields. Planet. Space Sci., **32**, 965–974.

[23] Langel, R.A. (1987) The Main Field. In J. Jacobs (ed.), Geomagnetism, 249–512, Academic Press, London.

[24] Langel, R.A., Estes, R.H. (1985) Large–Scale Near Field Magnetic Fields From External Sources and the Corresponding Induced Internal Field. J. Geoph. Res., **90**, 2487–2494.

[25] Langel, R.A. Sabaka, T.J., Baldwin, R.T., Conrad, J.A. (1996) The Near-Earth Magnetic Field from Magnetospherica and Quiet–day Ionospheric Sources and How it is Modelled. Physics of the Earth and Planetary Interiors, **98**, 235–267.

[26] Lühr, H., Warnecke, J., Rother, M. (1996) An Algorithm for Estimating Field–Aligned Currents from Single Spacecraft Magnetic Field Measurements: A Diagnostic Tool Applied to Freja Data. IEEE Traansactions on Geoscience and Remote Sensing, **34**, 1369–1376.

[27] Maier, T. (1999) Multiscale Analysis of the Geomagnetic Field. Diploma Thesis, University of Kaiserslautern, Geomathematics Group, .

[28] Maier, T., Bayer, M. (1998) Multiscale Analysis of the Geomagnetic Field. Progress in Geodetic Science at GW 98, 274-283 W. Freeden ed., Shaker-Verlag, Aachen.

[29] Olsen, N. (1997) Ionospheric F Region Currents at Middle and Low Latitudes Estimated From MAGSAT Data, J. Geophys. Res. **102**, 4563–4576.

[30] Olsen, W.P., Pfitzer, K.A. (1974) A Quantitative Model of the Magnetospheric Magnetic Field. J. Geophy. Res., **79**, 3739–3748.

[31] Richmond, A.D. (1974) The Computation of Magnetic Effects of Field–Aligned Magnetospheric Currents. J. Atmosph. and Terrestr. Phys., **36**, 245–252.

[32] Shure, L., Parker, R.L., Backus, G.E. (1982) Harmonic Splines for Geomagnetic Modelling. Phys. Earth Planet. Inst., **28**, 215–229.

[33] Stern, D.P. (1976) Representation of Magnetic Fields in Space. Rev. Geoph., **14**, 199-214.